Syntheses and ^{31}P NMR Studies of Cyclic Oxothiomolybdate(V) Molecular Rings: Exchange Properties and Crystal Structures of the Monophosphate Decamer $[(H_2PO_4)Mo_{10}S_{10}O_{10}(OH)_{11}(H_2O)_2]^{2-}$ and the Diphosphate Dodecamer $[(HPO_4)_2Mo_{12}S_{12}O_{12}(OH)_{12}(H_2O)_2]^{4-}$

Emmanuel Cadot, Bernadette Salignac, Thierry Loiseau, Anne Dolbecq, and Francis Sécheresse*[a]

Abstract: Solutions containing variable amounts of phosphate (noted P) and of $[Mo^{v}_{12}S_{12}O_{12}(OH)_{12}(H_2O)_6]$ (noted Mo_{12}) were studied by ^{31}P NMR spectroscopy. For $2 \le [P]/[Mo_{12}] \le 4$, $Na_4[(HPO_4)_2Mo_{12}S_{12}O_{12}(OH)_{12}(H_2O)_2]\cdot 27H_2O$ (**2**) was isolated in the solid state and fully characterized by X-ray diffraction study. Compound **2** crystallizes in the orthorhombic space group *Pnn*2 [$a = 17.712(3)$, $b = 19.092(3)$, $c = 11.135(1)$ Å]. The original Mo_{12} ring appears strongly deformed from circular to elliptical which illustrates the flexibility of the Mo skeleton under the phosphate addition. Such a result is explained by the pincer effect of the HPO_4^{2-} chelating groups supported by the mutual electrostatic repulsion between the two inner phosphato groups. Compound **2** exhibits a remarkable three-dimensional array resulting from connections between Na^+ and Mo_{12} polyanions forming 20-membered cavities stacked along pillars of sodium atoms. A complete ^{31}P NMR study of **2** in aqueous solution revealed that other species exist in solution, in equilibrium with **2**. For $[P]/[Mo_{12}] = 1$, orange crystals of $[N(CH_3)_4]_4Cl_{0.5}[Mo_{10}S_{10}O_{10}(OH)_{11}(H_2O)_4]_{0.5}$ $[(H_2PO_4)Mo_{10}S_{10}O_{10}(OH)_{11}(H_2O)_2]_{1.5}\cdot 16H_2O$ (**3**) were isolated. Compound **3** crystallizes in the triclinic $P\bar{1}$ space group [$a = 15.8972(2)$, $b = 18.0788(1)$, $c = 22.4694(2)$ Å, $\alpha = 94.71(1)$, $\beta = 90.26(1)$, $\gamma = 109.56(1)^\circ$]. The structure solution revealed two unexpected decameric rings, a monophosphato one $[(H_2PO_4)Mo_{10}S_{10}O_{10}(OH)_{11}(H_2O)_2]^{2-}$ and a phosphate-free one $[Mo_{10}S_{10}O_{10}(OH)_{11}(H_2O)_4]^{-}$. The effects of pH, temperature and concentrations ([P] and $[Mo_{12}]$) on the phosphate exchange properties of **2** were studied by ^{31}P NMR. The exchanges revealed to be slow enough on the NMR time scale to observe distinct resonances related to the presence of mono- and di-phosphato species.

Keywords: molybdenum · NMR · spectroscopy · polyoxometalates · sulfur · thiometalates

Introduction

Various aspects of the chemistry of the oxothiocation $[M^{V}_2S_2O_2]^{2+}$ M = Mo or W are currently under examination and numerous structures based on the $\{M_2S_2O_2\}$ core have been characterized, which differ in terms of the nature of the associated anionic ligand.[1] Fully sulfurated dianionic clusters containing terminal S_2^{2-} or S_4^{2-} ligands were used as starting materials for reactions involving ligand substitution.[2–6] For instance, Coucouvanis and Shibahara reported that terminal S_x^{2-} ligands could be substituted by various ligands such as sulfate, oxalate groups, and other organic ligands.[7–10] Recently, a one-dimensional (1D) polymeric compound was isolated resulting from the successive linear association of $\{Mo_2S_2O_2\}$ with As_2S_5 ligands.[11] However, most of these derivatives are dinuclear complexes and unlike the rich and varied chemistry of polyoxotungstates or -molybdates,[12] thio compounds are so far limited to small architectures containing reduced metal atoms. In previous work, we succeeded in introducing sulfur atoms in derived Keggin anions through the reaction between the preformed acid thio cation $[Mo_2S_2O_2]^{2+}$ and basic polyvacant anions such as γ-$[XW_{10}O_{36}]^{n-}$.[13] The resulting compounds have a very low sulfur content and exhibit molecular structures close to that of the polyoxometalate precursor. In a recent work, we reported a new strategy for the synthesis of such compounds based on the self-condensation of the thio precursor $[Mo_2O_2S_2]^{2+}$ by an acido-basic process. The first compound we described, a neutral molecular cluster $[Mo_{12}S_{12}O_{12}(OH)_{12}(H_2O)_6]$ (**1**) (Figure 1), results from the cyclic polymerization of the thio fragment at pH about 1.[14] The six $\{Mo_2S_2O_2\}$ building blocks are

[*] F. Sécheresse, E. Cadot, B. Salignac, T. Loiseau, A. Dolbecq
Institut Lavoisier. IREM, UMR C 0173
Université de Versailles Saint-Quentin
45 Avenue des Etats-Unis, F-78035 Versailles (France)
E-mail: secheres@chimie.uvsq.fr

0947-6539/99/0511-3390 $ 17.50+.50/0

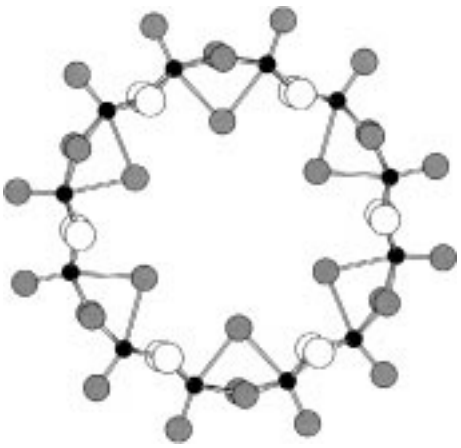

Figure 1. Molecular representation of $[Mo_{12}S_{12}O_{12}(OH)_{12}(H_2O)_6]$ (**1**). Mo^V centers are in black, S atoms are enlarged white spheres.

linked to each other through twelve hydroxo groups. A noteworthy feature of this neutral complex is the evidence of a central open cavity of about 11 Å in diameter lined with six water molecules, each Mo^V octahedron sharing alternatively edges (intra-building-block connections) and faces (inter-building-block connections). The condensation of $[Mo_2S_2O_2]^{2+}$ can be monitored in the presence of anionic structuring agent. With MoO_4^{2-}, the condensation gives the $[Mo_9S_8O_{11}(OH)_{10}(H_2O)]^{2-}$ ion, a mixed-valence octameric ring which encapsulates a Mo^{VI} octahedron.[15] Based on the same idea, we studied the influence of phosphate or arsenate ions on the polymerization of the thio precursor. For concentrated solutions of $H_2XO_4^-$ ions, the polycondensation quantitatively leads to the hexameric compounds $[(HXO_4)_4Mo_6S_6O_6(OH)_3]^{5-}$, X = As or P.[16] In those molecular anions, the connections between the three building blocks are exclusively edge-sharing. In solutions with a lower phosphate concentration, the neutral $[Mo_{12}S_{12}O_{12}(OH)_{12}(H_2O)_6]$ led to mono- and diphosphato anions. The diphosphato $[(HPO_4)_2Mo_{12}S_{12}O_{12}(OH)_{12}(H_2O)_2]^{4-}$ ion retains the original dodecameric structure and can be viewed as the first example illustrating the reactivity of the neutral $[Mo_{12}S_{12}O_{12}(OH)_{12}(H_2O)_6]$ wheel. The inner water molecules were labile enough to be substituted by phosphate ions which suggests that the cavity exhibits a real cationic character induced by the twelve Mo^V centers. For $[P]/[Mo_{12}] = 1$, the obtained monophosphato anion $[(H_2PO_4)Mo_{10}S_{10}O_{10}(OH)_{11}(H_2O)_2]^{2-}$ exhibits an unexpected decameric skeleton. We report here the ^{31}P NMR characterizations of those compounds in solution and propose an NMR assignment for the phosphato species.

Abstract in French: *Une étude par RMN de ^{31}P a été effectuée sur des solutions contenant des quantités variables d'ion phosphate (noté P) et de polyanion $[Mo^{v}_{12}S_{12}O_{12}(OH)_{12}(H_2O)_6]$ (noté Mo_{12}). Pour des rapports [P]/[Mo12] compris entre 2 et 4, le composé $Na_4[(HPO_4)_2Mo_{12}S_{12}O_{12}(OH)_{12}(H_2O)_2]\cdot 27H_2O$ (**2**) a été isolé à l'état solide et caractérisé par diffraction des rayons X sur monocristal. **2** cristallise dans le groupe d'espace orthorhombique Pnn2 [a = 17.712(3), b = 19.092(3), c = 11.1353(3) Å]. L'addition de phosphate se traduit par une déformation de la roue à 12 atomes de molybdène initiale, d'une géométrie circulaire à une géométrie elliptique, ce qui illustre la flexibilité du squelette métallique. La présence de deux groupements phosphate chélatants jouant le rôle de pinces, conjuguée à la répulsion électrostatique entre ces deux groupements, expliquent la déformation de la roue. La structure tridimensionnelle de **2** est remarquable : la connexion entre les ions sodium et les polyanions permet de dégager des cavités à 20 polyèdres, qui s'empilent le long des colonnes de sodium. Une étude complète par RMN d'une solution aqueuse de **2** a montré qu'il existait en solution d'autres espèces, en équilibre avec l'anion diphosphaté. Lorsque le rapport [P]/[Mo_{12}] est égal à 1, le composé $[N(CH_3)_4]_4Cl_{0.5}[Mo_{10}S_{10}O_{10}(OH)_{11}(H_2O)_4]_{0.5}[(H_2PO_4)Mo_{10}S_{10}O_{10}(OH)_{11}(H_2O)_2]_{1.5}\cdot 16H_2O$ (**3**) est isolé sous forme de cristaux oranges. **3** cristallise dans le groupe d'espace triclinique $P\bar{1}$ [a = 15.8972(2), b = 18.0788(1), c = 22.4694(2) Å, α = 94.71(1), β = 90.26(1), γ = 109.56(1)°]. L'analyse structurale a révélé la présence de roues diphosphatées à 10 atomes de molybdène, de formule $[(H_2PO_4)Mo_{10}S_{10}O_{10}(OH)_{11}(H_2O)_2]^{2-}$ ainsi que de roues sans phosphate $[Mo_{10}S_{10}O_{10}(OH)_{11}(H_2O)_4]^-$. L'effet du pH, de la température et des concentrations initiales ([P] et [Mo_{12}]) sur les propriétés d'échange de **2** ont également été étudiés par RMN. Les échanges entre les groupements phosphate et arsénate à l'intérieur de la roue sont suffisamment lents, à l'échelle de temps de la RMN, pour que l'on puisse observer les résonances correspondant aux différentes espèces.*

Results and Discussion

Molecular structure of $Na_4[(HPO_4)_2Mo_{12}S_{12}O_{12}(OH)_{12}(OH_2)_2]\cdot 27H_2O$ (2): The structure of $[(HPO_4)_2Mo_{12}S_{12}O_{12}(OH)_{12}(H_2O)_2]^{4-}$ (Figure 2) shows the $\{Mo_{12}S_{12}O_{12}(OH)_{12}\}$ cyclic skeleton of the precursor has been retained. Six $\{Mo_2O_2S_2\}$ units are doubly bridged through hydroxo groups. Two types of Mo–Mo distances are observed: short Mo–Mo distances (2.8002(6) – 2.8153(6) Å) within the $\{Mo_2O_2S_2\}$ building blocks characteristic of a metal – metal bond and long interblock Mo–Mo distances (3.226 – 3.299 Å). Two equivalent phosphate ions are symmetrically located in the central cavity. Each phosphate group is bonded to four adjacent Mo atoms through two equivalent P-O-Mo bridges. The two terminal P–O bonds of the phosphate groups are significantly different, the short value (1.423(9) Å) is characteristic of a P=O bond, while the longest one (1.576(8) Å) is consistent with a protonated oxygen atom.[17] The phosphorus tetrahedra are slightly displaced out of the Mo plane. The oxygen atom O5 of the P=O bond is located in the Mo plane, while the oxygen atom O15 of the P–OH bond occupies an out-of-plane position. As a consequence of the coordination of the two phosphates, the ring is distorted from circular to elliptical. This deformation is attributed to the electrostatic repulsion between the two diametrically opposite phosphate groups and is supported by the pincer effect of the two HPO_4^{2-} chelating groups. The Mo4-Mo5-Mo6 angle reflects this deformation, decreasing from 150° in the original wheel (**1**)[14] to 132°, while the Mo1-Mo2-Mo3 angle is increased to

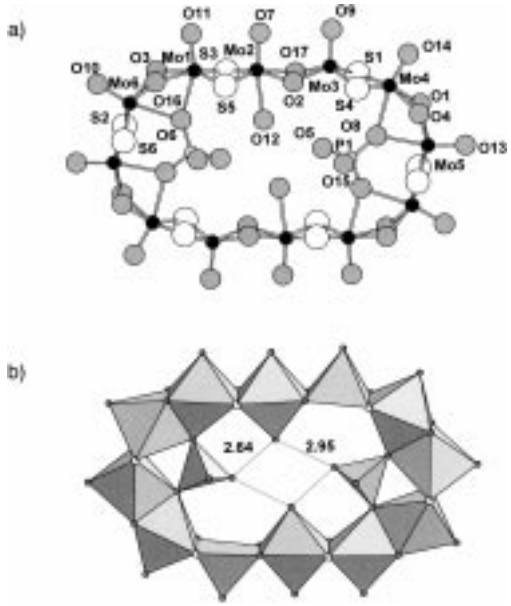

Figure 2. a) Molecular representation of $[(HPO_4)_2Mo_{12}S_{12}O_{12}(OH)_{12}(H_2O)_2]^{4-}$ (**2**). The patterns of the relevant atoms are identical to those in Figure 1. b) Polyhedral representation of the molecular structure of **2** with the hydrogen-bonding interactions between the P=O groups and the water molecules of the ring; the O···O distances [Å] are indicated next to the corresponding hydrogen bonds.

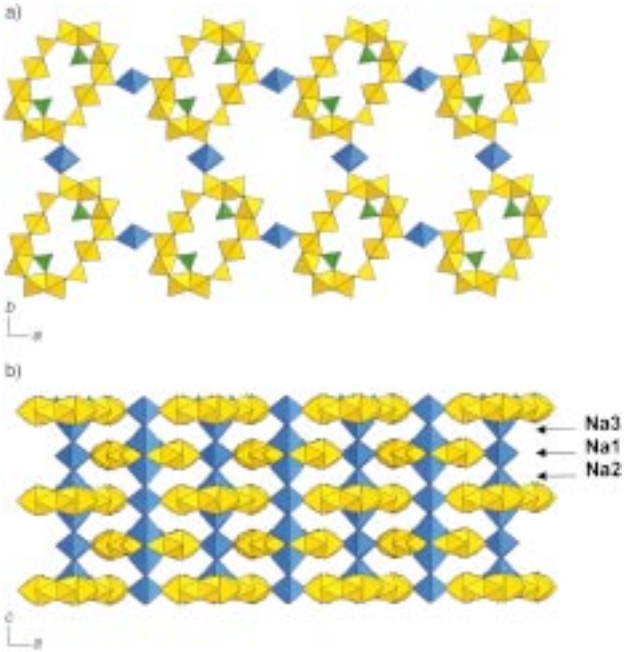

Figure 3. a) Polyhedral view of $Na_4[(HPO_4)_2Mo_{12}O_{12}S_{12}(OH)_{12}(H_2O)_2]\cdot 27H_2O$ (**2**) along the *c* axis. b) polyhedral view of **2** along the *b* axis, illustrating the pillared sodium atoms.

177°. Because of the opening of the Mo1-Mo2-Mo3 angle coupled with the steric constraint induced by the two phosphate groups of the cavity, a water molecule is displaced from Mo3 to Mo2 giving an octahedron at Mo2 and a pyramid at Mo3. The cohesion of the distorted dodecameric ring is supported by the existence of hydrogen bonds between the oxygen atom O5 of the deprotonated P=O bond and the oxygen atoms O12 of the inner water molecules (Figure 2b).

Three-dimensional structure of $Na_4[(HPO_4)_2Mo_{12}S_{12}O_{12}(OH)_{12}(OH_2)_2]\cdot 27H_2O$ (2): $Na_4[(HPO_4)_2Mo_{12}S_{12}O_{12}(OH)_{12}(OH_2)_2]\cdot 27H_2O$ exhibits a three-dimensional array in which cations and anions are mutually connected. Two views of the structure are given along the *c* axis and along the *b* axis in Figure 3a and 3b, respectively. All the Na^+ ions have octahedral environments formed by oxo ligands of the polyanion and by aqua ligands. Anions and Na1 cations form planes perpendicular to the crystallographic *c* axis. Each Na1 atom connects two anions through the terminal oxygen atom linked to Mo1, while the Na2 and Na3 atoms located on both sides of the plane are mutually edge-linked through the terminal oxygen atom of Mo4. The polyanion connections through Na^+ ions delimit large cavities of about 15 Å × 9 Å forming a 20-membered ring. Each plane is generated by a diagonal glide mirror, leading to the three-dimensional framework with a *c*/2 interplane distance. A nice feature of the structure is the presence of infinite sodium–oxygen chains running along the *c* axis. Edge-sharing Na^+ octahedra are linked by aqua and oxo ligands arranged in the following sequence: Na1(μ-OH_2)$_2$Na2(μ-O)$_2$Na3(μ-OH_2)$_2$Na1. The corresponding Na–Na distances are 3.62 Å, 4.00 Å, and 3.51 Å, respectively. The polyanions are distributed along the linear Na^+ pillars ensuring the cohesion of the array.

Molecular structure of $[N(CH_3)_4]_4Cl_{0.5}[Mo_{10}S_{10}O_{10}(OH)_{11}(H_2O)_4]_{0.5}[(H_2PO_4)Mo_{10}S_{10}O_{10}(OH)_{11}(H_2O)_2]_{1.5}\cdot 16H_2O$ (3): The structural analysis of **3** revealed the presence of four tetramethylammonium cations and two crystallographically independent anionic units, labeled A and B; an overall −2 charge was attributed to each anionic unit. The molecular structure of A is depicted in Figure 4a. Five $\{Mo_2O_2S_2\}$ building units, instead of six in the case of **1** and **2**, are connected to each other by hydroxo double bridges and form a decameric ring. A single phosphate group is present in the open cavity, slightly distorting it. The four Mo–O bonds between the Mo atoms of the ring and the oxygen atom of the phosphate group are not equivalent, three distances (2.281(9)–2.358(7) Å) are in the same range as those observed in the structure of **2** (2.323(3)–2.419(3) Å) but the Mo4A–O23A bond (3.009(8) Å) is significantly longer, so that O23A could be considered as a doubly bridging oxygen atom. The two terminal P–O bonds (1.56(1), 1.57(2) Å) are in the range of those observed for bridging dihydrogenophosphate groups.[18] The protonation of the two terminal P–O bonds is in agreement with the acidobasic properties of the monophosphato anion (as discussed below) and the pH of the synthesis solution of **3**. Among the three bridging oxygen atoms inside the cavity, two are assumed to be from water molecules and the other one from an hydroxo ligand in agreement with the −2 charge of anion A. Bond valence analysis[19] indicates that O22A is most likely the oxygen atom of this hydroxo ligand. On the basis of structural analysis, the detailed formula of anion A has thus been stated as $[(H_2PO_4)Mo_{10}S_{10}O_{10}(OH)_{11}(H_2O)_2]^{2-}$. At first sight, anion B has a molecular structure similar to that of anion A, however, unexpectedly, the occupancy factor of the phosphorus atom and of the two terminal oxygen atoms converged to 0.5, which means that a disorder can be postulated in the structure of

  0947-6539/99/0511-3392 $ 17.50+.50/0 *Chem. Eur. J.* **1999**, *5*, No. 11

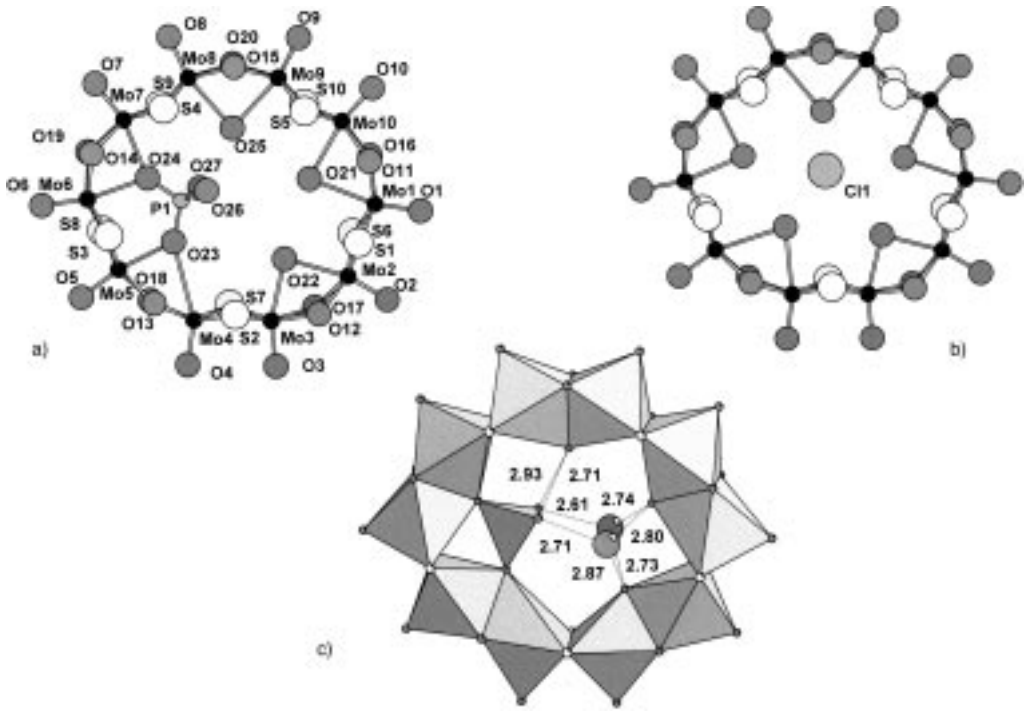

Figure 4. a) Molecular representation of $[(H_2PO_4)Mo_{10}S_{10}O_{10}(OH)_{11}(H_2O)_2]^{2-}$ present in A (occupancy factor 1.0) and in B (occupancy factor 0.5) in the structure of **3**. b) Molecular representation of $[Mo_{10}S_{10}O_{10}(OH)_{11}(H_2O)_2]^{-}$, present in B (occupancy factor 0.5) with the adjacent chlorine atom Cl1. c) Polyhedral representation of $[(H_2PO_4)Mo_{10}S_{10}O_{10}(OH)_{11}(H_2O)_2]^{2-}$ with the hydrogen-bonding pattern; the O···O distances [Å] are indicated next to the corresponding hydrogen bonds.

anion B. We have chosen to describe it as the superposition of two anions; the first one $[(H_2PO_4)Mo_{10}S_{10}O_{10}(OH)_{11}(H_2O)_2]^{2-}$ is identical to A (Figure 4a). The other one is a phosphate-free decamer in which the inner dihydrogenophosphate ligand has been replaced by two water molecules; a chlorine atom, with an occupancy factor of 0.5, balances the missing negative charge (Figure 4b). O22B can still be attributed to an hydroxo group so that the formula of the empty anionic ring is $[Mo_{10}S_{10}O_{10}(OH)_{11}(H_2O)_4]^{-}$. The chlorine atom is located at a distance of about 2.4 Å below the plane defined by the ten molybdenum atoms and is slightly off-center, a consequence of the electrostatic repulsion between the two electronegative entities Cl1 and O22B. In the phosphate containing anionic units A and B, the two terminal P–OH groups are hydrogen-bonded to two water molecules, located above and below the molecular plane, respectively, and to the oxygen atom O25 of the water molecule bridging Mo8 and Mo9. The resulting hydrogen-bonding pattern is shown in Figure 4c.

Infrared spectra: The IR spectrum of **2** exhibits two sets of intense absorptions at 953 and 919 cm^{-1} and at 553 and 497 cm^{-1}. The higher frequencies are attributed to ν(Mo=O) vibrations, the other set to the ν(Mo-OH-Mo) and ν(Mo-S-Mo) vibrations. These absorptions are characteristic of the oxo-thio metallic architecture and are located close to those of the free-phosphate wheel $[Mo_{12}S_{12}O_{12}(OH)_{12}(H_2O)_6]$ (**1**).[14] Additional medium absorptions are observed in the 1100–1000 cm^{-1} range, corresponding to the P–O stretching vibrations. Two bands and one shoulder are observed at 1152, 1034, and 1080 cm^{-1}, corresponding to the three expected asymmetric stretching modes for a PO_4 tetrahedron in low symmetry.

^{31}P MAS NMR spectroscopy: The ^{31}P MAS NMR spectrum of **2** exhibits a single isotropic line of resonance at $\delta = -4.0$. The symmetric pattern of the broad band ($\Delta\nu_{1/2} = 420$ Hz) confirms the presence of a unique site of phosphate in the solid state.

Synthesis: The diphosphato complex $[(HPO_4)_2Mo_{12}S_{12}O_{12}(OH)_{12}(H_2O)_2]^{4-}$ was obtained in the solid state as the sodium salt **2** by crystallization of solutions containing a suspension of the preformed wheel $[Mo_{12}S_{12}O_{12}(OH)_{12}(H_2O)_6]$,[14] to which $H_2PO_4^-$ ions were added (with $2 \le [P]/[Mo_{12}] \le 4$). Howeever, they can also be obtained by direct condensation of the $[Mo_2S_2O_2]^{2+}$ precursor by sodium hydroxide, in the presence of phosphate ions. Both resulting solutions exhibit at pH = 5 the same ^{31}P NMR spectrum and lead to the crystallization of **2** in comparable yield. For $[P]/[Mo_{12}] = 1$ and pH = 5.2, $[(H_2PO_4)Mo_{10}S_{10}O_{10}(OH)_{11}(H_2O)_2]^{2-}$ and $[Mo_{10}S_{10}O_{10}(OH)_{11}(H_2O)_4]^{-}$ ions co-crystallized in single crystals of $[N(CH_3)_4]_4Cl_{0.5}[Mo_{10}S_{10}O_{10}(OH)_{11}(H_2O)_4]_{0.5}$ $[(H_2PO_4)Mo_{10}S_{10}O_{10}(OH)_{11}(H_2O)_2]_{1.5} \cdot 16H_2O$ (**3**). As the tetramethylammonium cations come from the crude precursor $K_{2.6}(NMe_4)_{0.4}I_3[Mo_{12}S_{12}O_{12}(OH)_{12}(H_2O)_6] \cdot 30H_2O$,[14] the yield of the synthesis is very low. So far, our attempts to obtain these decameric anions as a pure crystalline salt, in a good yield, failed. Therefore, these results demonstrate that at least three compounds exist in solution, the free phosphate ions, the mono-, and diphosphate wheels, and their respective distribution depends on the $[P]/[Mo_{12}]$ ratio and the pH. The

number of protons on the phosphato species is obviously dependent on the pH value, and so, for clarity, except when necessary, protons attached to the polyanions and their charge will be omitted: thus, $[(HPO_4)_2Mo_{12}S_{12}O_{12}(OH)_{12}(H_2O)_2]^{4-}$ is noted P_2Mo_{12}, $[(H_2PO_4)Mo_{10}S_{10}O_{10}(OH)_{11}(H_2O)_2]^{2-}$, PMo_{10}, and $[Mo_{10}S_{10}O_{10}(OH)_{11}(H_2O)_4]^{-}$, Mo_{10}.

^{31}P NMR characterization of 2 in solution

Variable concentration: The effect of the concentration of **2** on the ^{31}P NMR spectra was studied at pH = 5.8 and T = 278 K. A set of spectra is given in Figure 5, revealing three main resonances noted δ_1, δ_2, and δ_3, located at $\delta = +1.05$, $\delta = -2.7$, and $\delta = -3.4$, respectively. A supplementary resonance is observed at about $\delta = -4$. Whatever the conditions,

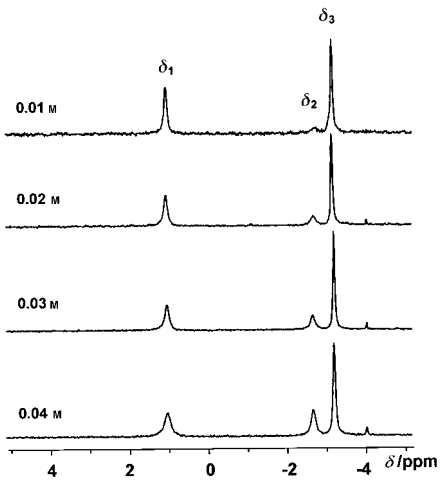

Figure 5. ^{31}P NMR spectra of aqueous P_2Mo_{12} solutions, with variable initial concentrations in P_2Mo_{12}, at 278 K.

its relative intensity is not higher than 2% and can be neglected with respect to the other three. When the concentration of **2** is increased, the relative intensity of δ_2 increases compared to the other two peaks, in agreement with the presence in solution of three phosphato species involved in the same equilibrium. By reference to $H_2PO_4^-$ solutions, the δ_1 peak is assigned to uncoordinated phosphate ions, while the two other lines, δ_2 and δ_3, correspond to linked phosphate groups. The relative intensity of the δ_2 resonance varies in the same way as the initial concentration and was assigned to the most condensed phosphato species, namely the diphosphato dodecamer P_2Mo_{12}. On this basis, the remaining δ_3 line is attributed to the monophosphato decamer PMo_{10}. The concentrations of each species were deduced from the relative intensities and the initial concentration of P_2Mo_{12} (Table 1). For all experiments, the free-phosphate wheel concentration remains close to zero and the $[PMo_{10}]/[P]$ ratios are in the 1.43–1.48 sharp range which corresponds to the theoretical value fixed by equilibrium (1). These results confirm that the system is well described by the preponderant equilibrium (1).

$$P_2Mo_{12} \rightleftharpoons 1.2\,PMo_{10} + 0.8\,P \quad (1)$$

Table 1. Data from ^{31}P NMR spectra with variable initial concentration in P_2Mo_{12}, at pH = 5.8 and T = 278 K.

$[P_2Mo_{12}]^0$ [mol L^{-1}]	0.040	0.030	0.020	0.015	0.010
relative intensity					
δ_1	0.31	0.33	0.35	0.36	0.37
δ_2	0.24	0.195	0.15	0.11	0.09
δ_3	0.45	0.475	0.50	0.53	0.54
concentration [M]					
[P]	0.025	0.020	0.014	0.011	0.007
$[P_2Mo_{12}]$	0.0096	0.0060	0.0030	0.0016	0.0009
$[PMo_{10}]$	0.036	0.028	0.020	0.016	0.011
apparent equilibrium constant	0.100	0.100	0.100	0.112	0.095

The related apparent constant is given by Equation (2) and the mean value $K = 0.1$ was deduced from the data collected at pH = 5.8 and T = 278 K.

$$K = \frac{[PMo_{10}]^{1.2}[P]^{0.8}}{[P_2Mo_{12}]} \quad (2)$$

We also studied the effect of the phosphate concentration on the relative intensities of the δ_1, δ_2, and δ_3 resonances. The variation of the $[P_2Mo_{12}]/[PMo_{10}]$ ratio with the initial $[P]^0/[Mo_{12}]^0$ ratio is shown in Figure 6. When the phosphate concentration increases the concentration of P_2Mo_{12} increases compared to that of PMo_{10}, in agreement with the previous assignment. The apparent constant K has been calculated from these data and has the same value $K = 0.1$.

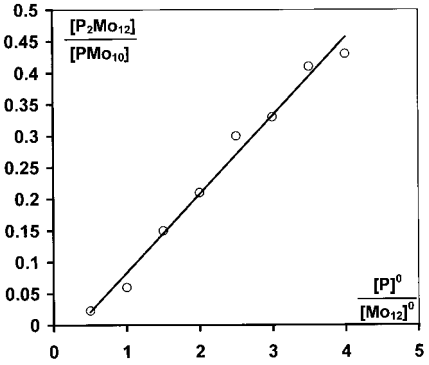

Figure 6. Dependence of the $[P_2Mo_{12}]/[PMo_{10}]$ ratio on the initial $[P]^0/[Mo_{12}]^0$ ratio, T = 278 K, $[P_2Mo_{12}]^0 = 0.04$ M.

Variable temperature: Selected ^{31}P NMR spectra of P_2Mo_{12}, recorded between 278 and 323 K are given in Figure 7. The ^{31}P NMR spectrum of P_2Mo_{12} in solution exhibits a strong temperature dependence, which is illustrated by the broadening of the three resonances. At 298 K, the δ_2 and δ_3 lines collapse to give a two broad-line spectrum, with $\Delta\nu_{1/2}$ = 120 Hz (at $\delta = 1.2$) for the uncoordinated phosphate and $\Delta\nu_{1/2} = 45$ Hz (at $\delta - 2.4$) for the mono- and diphosphato species. At 318 K, the δ_1 line disappears, while the width of the remaining resonance is enlarged to reach 200 Hz. Finally, at 323 K, a single broad line ($\Delta\nu_{1/2} = 420$ Hz) is observed at $\delta = -1.7$, resulting from the complete coalescence of the three initial resonances. These results agree with the existence of two independent dynamic exchanges in solution, one involving the phosphato groups linked to P_2Mo_{12} and uncoordinated

0947-6539/99/0511-3394 $ 17.50+.50/0 *Chem. Eur. J.* **1999**, *5*, No. 11

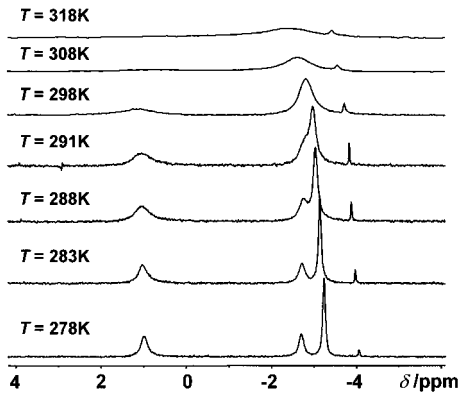

Figure 7. Variable-temperature ^{31}P NMR spectra of P_2Mo_{12} solutions, initial concentration $[P_2Mo_{12}]^0 = 0.04$ M.

phosphate ions, while the other one is related to PMo_{10} and uncoordinated phosphate ions. The overlapping of the δ_2 and δ_3 resonances is only due to the broadening of these two lines, through the two independent exchange processes.

^{31}P NMR characterization of mixtures of $[(HXO_4)_2Mo_{12}S_{12}O_{12}(OH)_{12}(H_2O)_2]^{4-}$, X = P or As: Selected ^{31}P NMR spectra of mixtures containing variable ratios of $[(HPO_4)_2Mo_{12}S_{12}O_{12}(OH)_{12}(H_2O)_2]^{4-}$ (P_2Mo_{12}) and $[(HAsO_4)_2Mo_{12}S_{12}O_{12}(OH)_{12}(H_2O)_2]^{4-}$ (As_2Mo_{12}) are shown in Figure 8. The diarsenato compound **4** is synthesized under

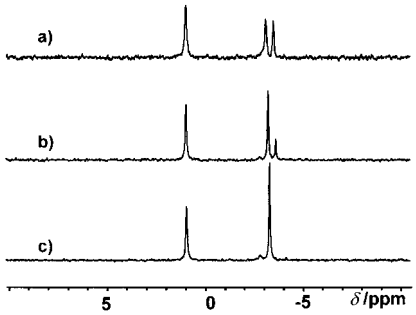

Figure 8. Phosphate–arsenate exchanges: ^{31}P NMR spectra of solutions with variable $[As_2Mo_{12}]^0/[P_2Mo_{12}]^0$ ratios; $[As_2Mo_{12}]^0/[P_2Mo_{12}]^0 = 4$ (a), $[As_2Mo_{12}]^0/[P_2Mo_{12}]^0 = 1$ (b), $[As_2Mo_{12}]^0/[P_2Mo_{12}]^0 = 0$ (c), for $([As_2Mo_{12}]^0 + [P_2Mo_{12}]^0) = 0.01$ M.

similar conditions to those used for the diphosphato compound **2**. The spectra of the mixtures are characterized by an additional resonance at $\delta = -3.6$ with an intensity ratio increasing with the amount of diarsenato polyanion (Figure 8). Such a result is explained by the formation of a new phosphato species, $PAsMo_{12}$, resulting from the phosphate–arsenate ion exchanges in the $\{Mo_{12}O_{12}S_{12}(OH)_{12}\}$ ring; this corresponds to equilibrium (3).

$$P_2Mo_{12} + As_2Mo_{12} \rightleftharpoons 2\,PAsMo_{12} \quad (3)$$

The resonance at $\delta = -3.6$, which is related to the mixed complex $PAsMo_{12}$, confirms the existence in solution of the X_2Mo_{12} anion (X = P, As). A second set of experiments was carried out consisting in the characterization of equimolar mixtures of P_2Mo_{12} and As_2Mo_{12} in variable concentrations ranging from 0.01 to 0.06 M. Selected spectra are reported in Figure 9. At low concentration (0.01 M), the line attributed to $PAsMo_{12}$, at $\delta = -3.6$, has a low intensity corresponding to about 15% of that of the monophosphato anion PMo_{10}, at $\delta = -2.82$. At this concentration, the line of the diphosphato

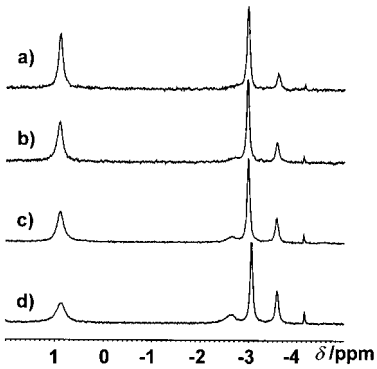

Figure 9. Phosphate–arsenate exchanges: ^{31}P NMR spectra of solutions with $[As_2Mo_{12}]^0/[P_2Mo_{12}]^0 = 1$ and variable ($[As_2Mo_{12}]^0 + [P_2Mo_{12}]^0$) (noted $[X_2Mo_{12}]^0$) concentrations; $[X_2Mo_{12}]^0 = 0.01$ M (a), $[X_2Mo_{12}]^0 = 0.02$ M (b), $[X_2Mo_{12}]^0 = 0.04$ M (c), $[X_2Mo_{12}]^0 = 0.06$ M (d).

anion P_2Mo_{12} is observed as a very weak and broad shoulder at $\delta = -2.5$. The intensities of the lines corresponding to $PAsMo_{12}$ and P_2Mo_{12} increase together with the concentration of the mixture and are approximately equal, leading to the ratio $[PAsMo_{12}]/[P_2Mo_{12}] = 2$. Such a value means that the arsenate and phosphate groups are statistically distributed in the $\{Mo_{12}O_{12}S_{12}(OH)_{12}\}$ wheel, which can be related to the very close chemical behavior of arsenate and phosphate ions.

pH dependence of the chemical shifts: The variation of δ_1, δ_2, and δ_3 chemical shifts with pH was studied at $T = 278$ K and is shown in Figure 10. The variation of δ_1 agrees with a monoprotonic exchange with a pK_a value of 6.3 corresponding to Equation (4). The variation of the δ_2 chemical shift indicates that one proton can be exchanged from the diphosphato ring P_2Mo_{12} ($pK_a = 6.5$) according to equilibrium (5). The curve representing the variation of δ_3 with pH is

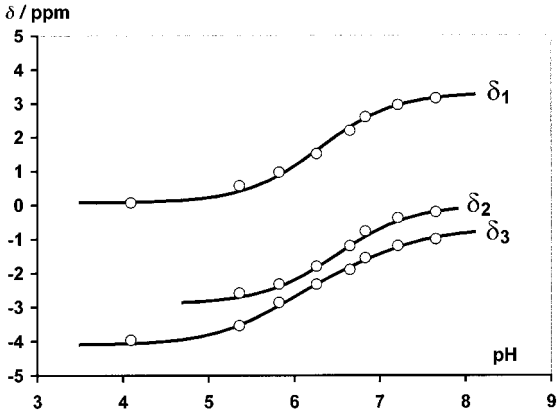

Figure 10. pH dependence of the experimental (points) and calculated (solid line) chemical shifts of the three phosphato species, $P(\delta_1)$, $PMo_{10}(\delta_3)$, and $P_2Mo_{12}(\delta_2)$.

in good agreement with that calculated for two successive proton exchanges with pK_a values of about 5.8 and 7.0. On the basis of our NMR attribution, the δ_3 resonance is due to the monophosphato anion PMo_{10}. Then, the two pK_a values correspond to the successive proton exchanges involved in equilibria (6) and (7).

$$H_2PO_4^- \rightleftharpoons HPO_4^{2-} + H^+ \quad (4)$$

$$[H_2P_2Mo_{12}]^{4-} \rightleftharpoons [HP_2Mo_{12}]^{5-} + H^+ \quad (5)$$

$$[H_2PMo_{10}]^{2-} \rightleftharpoons [HPMo_{10}]^{3-} + H^+ \quad (6)$$

$$[HPMo_{10}]^{3-} \rightleftharpoons [PMo_{10}]^{4-} + H^+ \quad (7)$$

Conclusion

The condensation of the oxothio fragment can be monitored by using an anionic structuring agent such as phosphate or arsenate ions. Depending on the concentration of the tetrahedral group, the assembling of the $\{Mo_2S_2O_2\}$ fragment leads to two sets of compounds. For solutions containing high concentrations of XO_4, X = As, P, the hexameric compounds $[(HXO_4)_4Mo_6S_6O_6(OH)_3]^{5-}$ resulting from edge-shared connections are obtained. For solutions with lower concentrations, the polymerization of the thio fragment leads to cyclic molecular rings based on face-shared connections. The presence of one or two phosphate chelating groups highlights the cationic character of the open cavity of the Mo_{10} or Mo_{12} rings, respectively. Due to their accessibility, the phoshate or arsenate groups can be easily exchanged through dynamic equilibria in solution. The deformation of the Mo skeleton from circular to elliptical under phosphate addition illustrates the flexibility of the molecular architecture favored by the versatility of the Mo^V atoms, which can adopt octahedral and pyramidal coordinations. ^{31}P NMR data and their interpretations lead one assign the observed resonances to the three phosphate species involved in the dynamic equilibria. This work can be extended to other assembling groups such as linear alkyl diphosphonates and dicarboxylates. Indeed the two independent tetrahedral groups in X_2Mo_{12} can be substituted by such bifunctional ligands. Preliminary experiments have shown that the length of the alkyl chain determines the nuclearity of the molecular ring.

Experimental Section

$Na_4[(HPO_4)_2Mo_{12}S_{12}O_{12}(OH)_{12}(H_2O)_2]\cdot 27H_2O$ (2): $K_{2,6}[NMe_4]_{0.4}[Mo_{12}S_{12}O_{12}(OH)_{12}(H_2O)_6]\cdot 30H_2O$[14] (1 g, 0.33 mmol) was hydrolyzed in HCl solution (10 mL, 4 M). Then $NaH_2PO_4\cdot 2H_2O$ (0.27 g, 1.73 mmol) was added and the pH was adjusted to 5 with NaOH (4 M). The solution was filtered and allowed to stand at room temperature for several days to give yellow-orange crystals (0.4 g, yield 44.3 %, based on Mo) suitable for X-ray determination. $Na_4[(HPO_4)_2Mo_{12}O_{12}S_{12}(OH)_{12}(H_2O)_2]\cdot 27H_2O$: calcd: Na 3.37, P 2.27, Mo 42.32, S 14.10; found: Na 3.39, P 2.18, Mo 40.24, S 14.07. Crystallization water was determined by thermogravimetric analysis (TGA) (up to 300 °C).

$[N(CH_3)_4]_4Cl_{0.5}[Mo_{10}S_{10}O_{10}(OH)_{11}(H_2O)_4]_{0.5}[(H_2PO_4)Mo_{10}S_{10}O_{10}(OH)_{11}(H_2O)_2]_{1.5}\cdot 16H_2O$ (3): $K_{2,6}[NMe_4]_{0.4}[Mo_{12}S_{12}O_{12}(OH)_{12}(H_2O)_6]\cdot 30H_2O$ (2 g, 0.66 mmol), $Na_2HPO_4\cdot 12H_2O$ (0.23 g, 0.66 mmol) and NaCl (0.25 g, 4.27 mmol) were dissolved in water (50 mL). The solution was allowed to stand at 5 °C for crystallization. After two weeks, well-shaped orange crystals of **3** were collected for single-crystal X-ray diffraction analysis.

$Na_4[(HAsO_4)_2Mo_{12}S_{12}O_{12}(OH)_{12}(H_2O)_2]\cdot 27H_2O$ (4): The synthetic procedure is similar to that of **2** except that $Na_2HAsO_4\cdot 6H_2O$ (0.5 g, 1.7 mmol) was used instead of NaH_2PO_4. $Na_4[(HAsO_4)_2Mo_{12}O_{12}S_{12}(OH)_{12}(H_2O)_2]\cdot 27H_2O$ (**4**): calcd: Na 3.25, As 5.30, Mo 40.76, S 13.59; found: Na 2.90, As 4.81, Mo 40.38, S 13.20. Crystallization water was determined by TGA (up to 300 °C). IR (cm^{-1}): $\tilde{\nu}$ = 958, 919 ν(Mo=O); 881, 827 ν(As–O); 494 ν(Mo-OH-Mo), ν(Mo-S-Mo); Compound **4** was characterized by the measurement of its cell parameters: monoclinic system, a = 17.9153(3), b = 19.3158(3), c = 11.2060(3) Å, and is isostructural to **2**.

Infrared spectra: IR spectra were recorded on a IRFT Magna 550 Nicolet spectrophotometer at 0.5 cm^{-1} resolution, using the technique of pressed KBr pellets.

NMR measurements: ^{31}P NMR spectra were recorded on a Bruker AC-300 spectrometer operating at 121.5 MHz in 5 mm tubes. ^{31}P chemical shifts are referenced to the external usual standard 85 % H_3PO_4. The pH dependence of the chemical shifts was studied by ^{31}P NMR at 278 K on solutions of **2** ($[P_2Mo_{12}] = 3.0\times10^{-2}$ M) with an ionic strength adjusted to I = 0.5 M by NaCl. The pH was adjusted by addition of NaOH or HCl (0.1 M).

Structure determination: Suitable parallelepiped-shaped orange crystals of **2** and **3** were selected for the crystal structure determination. Intensity data were recorded at room temperature on a Siemens SMART three-circle diffractometer equipped with a CCD bidimensional detector using the monochromated wavelength $\lambda(Mo_{K\alpha})$ = 0.71073 Å. An empirical correction was applied using the SADABS program[20] based on the method of Blessing.[21] The structure was solved by direct methods and refined by full-matrix least-squares using the SHELX-TL package.[22] The molybdenum, sulfur, and phosphorus atoms were located by direct methods and all the

Table 2. Crystallographic data for **2** and **3**.

	2	**3**
formula	$H_{72}Mo_{12}Na_4O_{61}P_2S_6$	$C_{16}H_{108}Mo_{20}N_4O_{66.5}P_3S_{20}$
M_r [g mol^{-1}]	2546.4	4037.2
color	orange	orange
crystal dimension [mm]	0.38 × 0.20 × 0.18	0.48 × 0.18 × 0.10
crystal system	orthorombic	triclinic
space group	*P*nn2 (no. 34)	$P\bar{1}$ (no. 2)
T [K]	296	296
a [Å]	17.712(3)	15.8972(2)
b [Å]	19.092(3)	18.0788(1)
c [Å]	11.135(1)	22.4694(2)
α [°]	90	94.71(1)
β [°]	90	90.26(1)
γ [°]	90	109.56(1)
V [Å^3]	3765.5(9)	6060.9(1)
Z	2	2
ρ_{calcd} [g cm^{-3}]	2.273	2.217
μ [mm^{-1}]	2.410	2.445
θ range [°]	3.40 – 32.50	0.91 – 29.62
reflections measured	30346	41181
unique reflections (R_{int})	12498 (0.0247)	29316 (0.0418)
observed ($I > 2\sigma(I)$)	9827	13152
refined parameters	330	1075
$R_1(F)$[a]	0.0373	0.0628
$wR_2(F^2)$[b]	0.1146	0.1449
$\Delta\rho$(max/min) [e Å^{-3}]	2.63 and −1.14	3.66[c] and −1.16

[a] $R_1 = \frac{\sum||F_o|-|F_c||}{\sum|F_c|}$. [b] $wR_2 = \sqrt{\frac{\sum w(F_o^2-F_c^2)^2}{\sum w(F_o^2)^2}}$, $1/w = \sigma^2F_o^2 + (aP)^2 + bP$, $P = \frac{F_o^2+2F_c^2}{3}$, and a = 0.0747, b = 7.2699 for **2**; a = 0.0891, b = 31.4862 for **3**. [c] The residual density was found near the disordered phosphate group of anion B.

0947-6539/99/0511-3396 $ 17.50+.50/0 *Chem. Eur. J.* **1999**, *5*, No. 11

Table 3. Selected bond lengths [Å] in **2** and **3**.

2									
Mo1–O11	1.683(4)	Mo1–O3	2.120(7)	Mo1–O16	2.142(8)	Mo1–S5	2.320(3)	Mo1–O6	2.323(3)
Mo1–S3	2.324(3)	Mo1–Mo2	2.8002(6)	Mo2–O7	1.693(4)	Mo2–O2	2.072(7)	Mo2–O17	2.109(8)
Mo2–S3	2.297(3)	Mo2–O12	2.310(4)	Mo2–S5	2.321(3)	Mo3–O9	1.685(4)	Mo3–O17	2.018(8)
Mo3–O2	2.083(7)	Mo3–S4	2.296(3)	Mo3–S1	2.297(3)	Mo3–Mo4	2.8153(6)	Mo4–O14	1.693(4)
Mo4–O4	2.067(7)	Mo4–O1	2.140(8)	Mo4–S1	2.314(3)	Mo4–S4	2.320(3)	Mo4–O8	2.365(3)
Mo5–O13	1.687(4)	Mo5–O4	2.075(8)	Mo5–O1	2.123(8)	Mo5–S6	2.301(4)	Mo5–S2	2.333(3)
Mo5–O8	2.362(3)	Mo5–Mo6	2.8105(6)	Mo6–O10	1.685(4)	Mo6–O16	2.085(9)	Mo6–O3	2.108(7)
Mo6–S2	2.322(4)	Mo6–S6	2.324(4)	Mo6–O6	2.419(3)	P1–O5	1.423(9)	P1–O8	1.535(4)
P1–O6	1.538(4)	P1–O15	1.576(8)						
3									
Anion A									
Mo1A–O1A	1.699(8)	Mo1A–O16A	2.104(8)	Mo1A–O11A	2.115(8)	Mo1A–S1A	2.329(3)	Mo1A–S6A	2.333(3)
Mo1A–O21A	2.600(8)	Mo1A–Mo2A	2.855(2)	Mo2A–O2A	1.695(8)	Mo2A–O17A	2.123(8)	Mo2A–O12A	2.123(9)
Mo2A–S6A	2.334(3)	Mo2A–S1A	2.328(3)	Mo2A–O22A	2.442(10)	Mo3A–O3A	1.701(10)	Mo3A–O12A	2.129(8)
Mo3A–O17A	2.126(9)	Mo3A–S2A	2.341(4)	Mo3A–O22A	2.345(10)	Mo3A–S7A	2.348(3)	Mo3A–Mo4A	2.853(2)
Mo4A–O4A	1.667(10)	Mo4A–O13A	2.071(8)	Mo4A–O18A	2.087(9)	Mo4A–S7A	2.331(3)	Mo4A–S2A	2.333(4)
Mo4A–O23A	3.009(11)	Mo5A–O5A	1.710(9)	Mo5A–O13A	2.112(8)	Mo5A–O18A	2.124(9)	Mo5A–O23A	2.281(9)
Mo5A–S3A	2.330(4)	Mo5A–S8A	2.337(3)	Mo5A–Mo6A	2.854(2)	Mo6A–O6A	1.693(8)	Mo6A–O19A	2.106(9)
Mo6A–O14A	2.128(9)	Mo6A–S3A	2.335(4)	Mo6A–S8A	2.349(3)	Mo6A–O24A	2.358(7)	Mo7A–O7A	1.701(10)
Mo7A–O19A	2.131(8)	Mo7A–O14A	2.129(8)	Mo7A–O24A	2.336(8)	Mo7A–S4A	2.336(3)	Mo7A–S9A	2.348(3)
Mo7A–Mo8A	2.852(2)	Mo8A–O8A	1.684(9)	Mo8A–O20A	2.114(8)	Mo8A–O15A	2.132(8)	Mo8A–S4A	2.327(4)
Mo8A–S9A	2.337(3)	Mo8A–O25A	2.475(10)	Mo9A–O9A	1.680(9)	Mo9A–O15A	2.111(7)	Mo9A–O20A	2.124(8)
Mo9A–S5A	2.331(3)	Mo9A–S10A	2.334(3)	Mo9A–O25A	2.510(9)	Mo9A–Mo10A	2.8492(14)	Mo10A–O10A	1.672(9)
Mo10A–O11A	2.108(8)	Mo10A–O16A	2.123(8)	Mo10A–S5A	2.341(3)	Mo10A–S10A	2.339(3)	Mo10A–O21A	2.442(8)
P1A–O24A	1.502(8)	P1A–O27A	1.558(14)	P1A–O26A	1.57(2)	P1A–O23A	1.549(12)		
Anion B									
Mo1B–O1B	1.675(9)	Mo1B–O16B	2.112(7)	Mo1B–O11B	2.131(8)	Mo1B–S1B	2.327(3)	Mo1B–S6B	2.340(3)
Mo1B–O21B	2.462(9)	Mo1B–Mo2B	2.8475(14)	Mo2B–O2B	1.695(8)	Mo2B–O17B	2.122(7)	Mo2B–O12B	2.131(8)
Mo2B–O22B	2.337(8)	Mo2B–S6B	2.338(3)	Mo2B–S1B	2.343(3)	Mo3B–O3B	1.687(8)	Mo3B–O17B	2.133(8)
Mo3B–O12B	2.137(8)	Mo3B–O22B	2.278(8)	Mo3B–S2B	2.339(3)	Mo3B–S7B	2.340(3)	Mo3B–Mo4B	2.8388(14)
Mo4B–O4B	1.701(8)	Mo4B–O18B	2.100(7)	Mo4B–O13B	2.109(8)	Mo4B–S2B	2.335(3)	Mo4B–S7B	2.347(3)
Mo4B–O28B	2.56(2)	Mo5B–O5B	1.691(9)	Mo5B–O13B	2.114(8)	Mo5B–O18B	2.129(7)	Mo5B–O23B	2.31(2)
Mo5B–S8B	2.337(3)	Mo5B–S3B	2.341(3)	Mo5B–Mo6B	2.8589(13)	Mo6B–O6B	1.691(9)	Mo6B–O14B	2.107(7)
Mo6B–O19B	2.127(7)	Mo6B–S3B	2.336(3)	Mo6B–S8B	2.348(3)	Mo6B–O24B	2.371(8)	Mo7B–O7B	1.693(8)
Mo7B–O14B	2.132(7)	Mo7B–O19B	2.125(7)	Mo7B–S9B	2.341(3)	Mo7B–O24B	2.339(8)	Mo7B–S4B	2.341(3)
Mo7B–Mo8B	2.8423(14)	Mo8B–O8B	1.686(7)	Mo8B–O15B	2.100(8)	Mo8B–O20B	2.110(8)	Mo8B–S4B	2.324(3)
Mo8B–S9B	2.332(3)	Mo8B–O25B	2.597(8)	Mo9B–O9B	1.687(8)	Mo9B–O15B	2.112(8)	Mo9B–O20B	2.111(8)
Mo9B–S5B	2.336(3)	Mo9B–S10B	2.353(3)	Mo9B–O25B	2.553(9)	Mo9B–Mo10B	2.8594(14)	Mo10B–O10B	1.695(9)
Mo10B–O16B	2.112(7)	Mo10B–O11B	2.132(7)	Mo10B–S5B	2.339(3)	Mo10B–S10B	2.350(3)	Mo10B–O21B	2.391(8)
P1B–O26B	1.56(2)	P1B–O24B	1.560(10)	P1B–O23B	1.57(2)	P1B–O27B	1.657(12)		

non-hydrogen atoms were placed from subsequent Fourier difference map calculations. In the structure of **2**, among the four expected sodium cations obtained by elemental analysis, only three were located. Among the 27 water molecules of crystallization determined from the thermogravimetric analysis, 21 were located. The missing sodium and water molecules are assumed to be delocalized in the structure and were not placed in the refinement. In the structure of **3**, the asymmetric unit contains two anionic rings labeled A and B which encapsulate a single phosphate group. In ring A the phosphorus atom has a full occupancy, while in ring B the refinement of the occupancy factor of the phosphorus atom converged to 0.47 and was subsequently set to 0.5. A chlorine atom with an occupancy factor of 0.5 was found in the Fourier difference map and compensates the missing 0.5 negative charge. The oxygen atom O23 in ring B is also disordered over two positions (O23B and O28B). All the atoms of the polyanions, the sodium atoms in **2**, as well as the atoms of the tetramethylammonium cations in **3** were refined anisotropically, while the disordered atoms in **3** and the oxygen atoms of the water molecules were refined by using isotropic temperature factors. Crystal data and details of the data collection are summarized in Table 2. Selected bond lengths are reported in Table 3. Further details on the crystal structure investigation(s) may be obtained from the Fachinformationszentrum Karlsruhe, D-76344 Eggenstein-Leopoldshafen, Germany (fax: (+49) 7247-808-666); e-mail: crysdata@fiz-karlsruhe.de), on quoting the depository numbers CSD-410038 for **2** and CSD-410756 for **3**.

Acknowledgment

We thank Marie Josée Pouet and Chantal Labarre from SIRCOB (Université de Versailles, France) for helpful discussion about ^{31}P NMR spectra in solution. Jocelyne Maquet from LCMC (Université Pierre et Marie Curie, France) is gratefully acknowledged for recording the ^{31}P MAS NMR spectra.

[1] See for a review : T. Shibahara, *Coord. Chem. Rev.* **1993**, *123*, 73–147.
[2] R. Bhattacharyya, P. K. Chakrabarty, P. N. Ghosh, A. K. Mukherjee, D. Podder, M. Mukherjee, *Inorg. Chem.* **1991**, *30*, 3948.
[3] S. Sakar, M. A. Ansari, *J. Chem. Soc. Chem. Commun.* **1986**, 324.
[4] A. Müller, W. Rittner, A. Neumann, R. C. Sharma, *Z. Anorg. Allg. Chem.* **1981**, *472*, 69.
[5] W. Rittner, A. Müller, A. Neumann, W. Bather, R. C. Sharma, *Angew. Chem.* **1979**, *91*, 565; *Angew. Chem. Int. Ed. Engl.* **1979**, *18*, 530.
[6] A. Müller, E. Krickemeyer, U. Reinsch, *Z. Anorg. Allg. Chem.* **1980**, *470*, 35.
[7] D. Coucouvanis, A. Toupadakis, A. Hadjikyriacou, *Inorg. Chem.* **1988**, *27*, 3272.
[8] D. Coucouvanis, A. Toupadakis, J. D. Lane,S. M. Koo, C. G. Kim, A. J. Hadjikyriacou, *J. Am. Chem. Soc.* **1991**, *113*, 5271.

  0947-6539/99/0511-3397 $ 17.50+.50/0

[9] F. A. Armstrong, T. Shibahara, A. G. Sykes, *Inorg. Chem.* **1978**, *17*, 189.
[10] G. Chang, D. Coucouvanis, *Inorg. Chem.* **1993**, *32*, 2232.
[11] J.-H. Chou, J. A. Hanko, M. G. Kanatzidis, *Inorg. Chem.* **1997**, *36*, 4.
[12] A. Müller, F. Peters, M. Pope, D. Gatteschi, *Chem. Rev.* **1998**, *98*, 239.
[13] a) E. Cadot, V. Béreau, B. Marg, S. Halut, F. Sécheresse, *Inorg. Chem.* **1996**, *25*, 3099; b) E. Cadot, V. Béreau, F. Sécheresse, *Inorg. Chim. Acta* **1996**, *252*, 101.
[14] E. Cadot, B. Salignac, S. Halut, F. Sécheresse, *Angew. Chem.* **1998**, *110*, 631; *Angew. Chem. Int. Ed.* **1998**, *37*, 611.
[15] A. Dolbecq, B. Salignac, E. Cadot, F. Sécheresse, *Bull. Pol. Acad. Sci.* **1998**, *46*, 237.
[16] E. Cadot, A. Dolbecq, B. Salignac, F. Sécheresse, *Chem. Eur J.* **1999**, *5*, 2396.
[17] M. I. Khan, Q. Chen, J. Zubieta, *Inorg. Chim. Acta* **1995**, *235*, 135.
[18] W. T. A. Harrison, L. Hannooman, *J. Solid State Chem.* **1997**, *131*, 363.
[19] N. E. Brese and M. O'Keeffe, *Acta Crystallogr. B* **1991**, *47*, 192.
[20] G. M. Sheldrick, a program for the Siemens area detector absorption correction, Universität Göttingen, Germany, **1997**.
[21] R. Blessing, *Acta Crystallogr. A* **1995** *51*, 33.
[22] G. M. Sheldrick , SHELX-TL version 5.03, Software Package for the Crystal Structure Determination Siemens Analytical X-ray Instruments Inc. Madison, Wisconsin USA, **1994**.

Received: August 5, 1998
Revised version: March 20, 1999 [F 1287]

  0947-6539/99/0511-3398 $ 17.50+.50/0